Theoret. Chim. Acta (Berl.) 32, 187–201 (1974)

Commentationes

An MO Study of Bridge Bonds in B_2H_6

Shinichi Yamabe, Tsutomu Minato, Hiroshi Fujimoto, and Kenichi Fukui
Faculty of Engineering, Kyoto University, Sakyo-ku, Kyoto, Japan

Received May 7/August 20, 1973

An *ab initio* molecular orbital calculation is carried out on diborane (B_2H_6). Regarding B_2H_6 as an interacting system of two BH_3, we investigate the charge density in the area between these BH_3 within the framework of *configuration analysis*. The charge transfer interaction is found to be most important for the proper description of the bridged three-center bonds in B_2H_6.

Key words: Diborane – Bridge structure

1. Introduction

The electronic structure of boron hydrides has received an appreciable attention in a number of theoretical works [1–4]. Among the compounds, diborane is a typical and the simplest electron-deficient molecule, which gives us the knowledge about its molecular properties and its electronic structure, particularly in terms of the molecular orbital (MO) method [5–11]. Buenker and coworkers suggested why it prefers the bridged D_{2h} structure to the D_{3d} staggered configuration favored by ethane, following substantially the rule of Walsh [7]. Another striking way to approach the electronic structural problem can be seen in the report dealing with the MO's in the localized form because the usual *delocalized* MO's somewhat lack in the information of the chemical feature about three-center bridge bonds [12, 13].

Gelus *et al.* pointed out the important role of the correlation energy to the binding energy in the dimerization process of two boranes to diborane. This result seems to give warning to the usual method to predict the energy terms by the *ab initio* MO on the Hartree-Fock level, especially in such a case that the product, B_2H_6, has *abnormal* three-center bonds [14].

Here, the present work is not discussed from energetic point of view, but intended to show a *new* chemical idea why the stable structure of diborane is given in D_{2h} symmetry in the frame of the MO language using the concept of the orbital interaction. In this treatment the diborane molecule is regarded as the "complex" compound of two unstable molecular fragments, $(BH_3)_2$, reflecting the experimental results as to the self-associated reaction of two boranes [15, 16]. This intentional decomposition of B_2H_6 into two deformed BH_3 gives permission to use *configuration analysis* [17–19] which expresses the notion of the orbital interaction most directly. By the employment of the technique, the electron density at the central region in the diborane molecule, which is the origin of this *abnormal* bond, is analyzed.

In short, we detect the source to make the bridged structure in B_2H_6 stable by dividing it into the interacting two subsystems.

2. MO Calculation

The MO's necessary to our discussion are obtained by the usual SCF (Self-Consistent-Field) procedure [20] with the minimal basis set of Slater Type Orbitals (STO's), of which the exponent, ζ, is that given by Pople *et al.* [21]. The STO is expanded into *three* Gaussian Type Orbitals (GTO's) [22, 23] for the easiness of the computation of several integrals (STO-3G). The exponent, α_i, and the coefficient, c_i, of the GTO's are taken from Stewart's result [24].

$$\mathrm{STO}(\zeta) = \sum_{i=1}^{3} c_i \,\mathrm{GTO}(\alpha_i)\,. \tag{1}$$

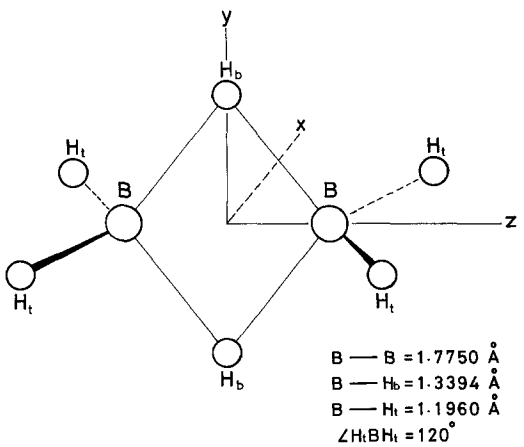

Fig. 1. The geometry of B_2H_6 taken in this calculation

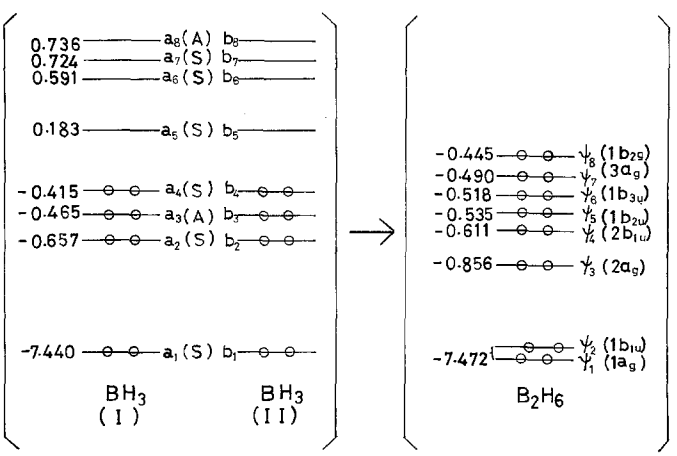

Fig. 2. The MO's of two deformed BH_3 at the left side and those of B_2H_6 at the right. The orbital energies are in atomic unit. The unoccupied MO's of B_2H_6 are not shown here because they are unnecessary for our discussion

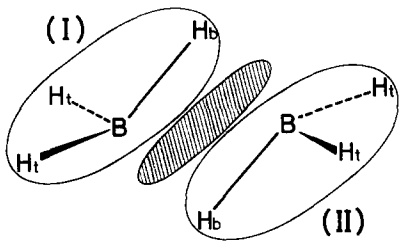

Fig. 3. The systematic representation of the *interacting* two fragmental BH_3 in B_2H_6

In this calculation B_2H_6 is assumed to have D_{2h} symmetry, and the experimental geometry by Bartell and Carroll [25] was used as pictured in Fig. 1, where H_b means a bridge hydrogen atom located in $y-z$ plane and H_t is a terminal hydrogen in $x-z$ plane. With respect to the geometry adopted in Fig. 1, the occupied MO's of diborane (Ψ_g, $g=1, 2, \ldots, 8$) are given[1] in the right hand of Fig. 2 where the order of the symmetry orbitals ($1a_g$, $1b_u$, $2a_g$, ...) agrees with the result by Lipscomb *et al.* [10].

The method of the configuration analysis needs also the MO's of two deformed BH_3, which construct the B_2H_6 structure, tentatively termed (I) and (II). The computed results of them are displayed in the left hand of Fig. 2. The occupied MO's in one fragment (I) are defined $a_i (i=1, 2, 3, 4)$ and the unoccupied ones $a_j (j=5, 6, 7, 8)$, while the occupied MO's in the other fragment (II) are named $b_k (k=1, 2, 3, 4)$ and the vacant ones $b_l (l=5, 6, 7, 8)$. Accordingly, a_i is equivalent to b_k in $i=k$ and a_j to b_l in $j=l$. The symmetry signs (A and S) attached to the MO's of two BH_3 are according to whether the MO is symmetry (S) or *anti*-symmetry (A) with respect to the $y-z$ plane (see Fig. 1).

Hereunto the results of the MO properties have been prepared on diborane and its subsystems, (I) and (II), available for our later purpose. In Fig. 3 the schematic representation of the *interacting* two fragmental BH_3 in diborane is shown. The shaded part in this figure means the intermolecular region regarding the two entities.

3. Description of Method

First the occupied MO of diborane (Ψ_g) is approximated by a linear combination of the MO's belonging to the two fragments (LCMO);

$$\Psi_g = \sum_{f=1}^{16} d_f^{(g)} \Phi_f \qquad (g=1, 2, \ldots, 8), \tag{2}$$

where g is the suffix attached to the MO of diborane and runs from 1 to 8, namely 8 is the number of the occupied MO's in diborane. There, Φ_f is the *local* MO of two fragments in Fig. 2. That is, Φ_f is the general notation for the respective

[1] The effect of the *correlation energy* [14] was estimated by taking into account the contribution of the doubly-excited state to the stabilization (ΔE) of the system. As a result of the evaluation ($\Delta E = 0.793$ eV), our later discussion is thought to be insensitive to whether the effect is included or not.

MO's in two systems;

$$\Phi_f : (a_1, a_2, \ldots, a_i, \ldots, a_j, \ldots, a_8, b_1, \ldots, b_k, \ldots, b_l, \ldots, b_8)\,. \tag{3}$$

In Eq. (2) $d_f^{(g)}$ is the expansion coefficient attached to the f-th MO in the fragmental systems. When Φ_f is replaced by a_i, a_j, b_k, and b_l in Eq. (3), Eq. (2) is rewritten by the following equation;

$$\Psi_g = \sum_{i=1}^{4} d_i^{(g)} a_i + \sum_{j=5}^{8} d_j^{(g)} a_j + \sum_{k=1}^{4} d_{k+8}^{(g)} b_k + \sum_{l=5}^{8} d_{l+8}^{(g)} b_l\,. \tag{4}$$

That is, Eq. (4) shows the relationship between the MO's of the two subsystems and the MO of diborane.

Then the electron density $\{\varrho(1\,|\,1)\}$ in B_2H_6, originally defined by Ψ_g, can be decomposed into several fragmental parts [18] by the use of Eq. (4);

$$\begin{aligned}
\varrho(1\,|\,1) &= 2\sum_{g=1}^{8} \Psi_g^2(1) \\
&= 2\sum_{g=1}^{8}\Bigg[\sum_{i=1}^{4}\{d_i^{(g)} a_i(1)\}^2 + \sum_{j=5}^{8}\{d_j^{(g)} a_j(1)\}^2 \\
&\quad + \sum_{k=1}^{4}\{d_{k+8}^{(g)} b_k(1)\}^2 + \sum_{l=5}^{8}\{d_{l+8}^{(g)} b_l(1)\}^2\Bigg] \\
&\quad + 2\sum_{g=1}^{8}\Bigg[\sum_{i=1}^{4}\sum_{i'(>i)}^{4} d_i^{(g)} d_{i'}^{(g)}\{a_i(1)\,a_{i'}(1) + a_{i'}(1)\,a_i(1)\} \\
&\quad + \sum_{i=1}^{4}\sum_{j=5}^{8} d_i^{(g)} d_j^{(g)}\{a_i(1)\,a_j(1) + a_j(1)\,a_i(1)\} \\
&\quad + \sum_{j=5}^{8}\sum_{j'(>j)}^{8} d_j^{(g)} d_{j'}^{(g)}\{a_j(1)\,a_{j'}(1) + a_{j'}(1)\,a_j(1)\}\Bigg] \\
&\quad + 2\sum_{g=1}^{8}\Bigg[\sum_{k=1}^{4}\sum_{k'(>k)}^{4} d_{g+8}^{(g)} d_{k'+8}^{(g)}\{b_k(1)\,b_{k'}(1) + b_{k'}(1)\,b_k(1)\} \\
&\quad + \sum_{k=1}^{4}\sum_{l=5}^{8} d_{k+8}^{(g)} d_{l+8}^{(g)}\{b_k(1)\,b_l(1) + b_l(1)\,b_k(1)\} \\
&\quad \sum_{l=5}^{8}\sum_{l'(>l)}^{8} d_{l+8}^{(g)} d_{l'+8}^{(g)}\{b_l(1)\,b_{l'}(1) + b_{l'}(1)\,b_l(1)\}\Bigg] \\
&\quad + 2\sum_{g=1}^{8}\Bigg[\sum_{i=1}^{4}\sum_{k=1}^{4} d_i^{(g)} d_{k+8}^{(g)}\{a_i(1)\,b_k(1) + b_k(1)\,a_i(1)\} \\
&\quad + \sum_{i=1}^{4}\sum_{l=5}^{8} d_i^{(g)} d_{l+8}^{(g)}\{a_i(1)\,b_l(1) + b_l(1)\,a_i(1)\} \\
&\quad + \sum_{j=5}^{8}\sum_{k=1}^{4} d_j^{(g)} d_{k+8}^{(g)}\{a_j(1)\,b_k(1) + b_k(1)\,a_j(1)\} \\
&\quad + \sum_{j=5}^{8}\sum_{l=5}^{8} d_j^{(g)} d_{l+8}^{(g)}\{a_j(1)\,b_l(1) + b_l(1)\,a_j(1)\}\Bigg]
\end{aligned} \tag{5}$$

This procedure means that the electron density in B_2H_6 is regarded as the quantity yielded by the orbital *mixing* between two borane components. Equation (5) allows the systematic partitioning of the density by the delocalized MO, i.e. Ψ_g.

Here in order to investigate some components in Eq. (5), five quantities are newly defined by the abstraction of the cross terms such as $a_i(1)\,b_k(1)$ from the Equation.

$$\varrho(1\,|\,1)_{\text{total}} = \varrho(1\,|\,1)_{\text{exchange}} + \varrho(1\,|\,1)_{\text{CT}} + \varrho(1\,|\,1)_{\text{back CT}} + \varrho(1\,|\,1)_{j,l}\,, \tag{6}$$

where

$$\varrho(1\,|\,1)_{\text{exchange}} = 2\sum_{g=1}^{8}\left[\sum_{i=1}^{4}\sum_{k=1}^{4} d_i^{(g)}\,d_{k+8}^{(g)}\,\{a_i(1)\,b_k(1) + b_k(1)\,a_i(1)\}\right], \tag{7}$$

$$\varrho(1\,|\,1)_{\text{CT}} = 2\sum_{g=1}^{8}\left[\sum_{i=1}^{4}\sum_{l=5}^{8} d_i^{(g)}\,d_{l+8}^{(g)}\,\{a_i(1)\,b_l(1) + b_l(1)\,a_i(1)\}\right], \tag{8}$$

$$\varrho(1\,|\,1)_{\text{back CT}} = 2\sum_{g=1}^{8}\left[\sum_{j=5}^{8}\sum_{k=1}^{4} d_j^{(g)}\,d_{k+8}^{(g)}\,\{a_j(1)\,b_k(1) + b_k(1)\,a_j(1)\}\right], \tag{9}$$

$$\varrho(1\,|\,1)_{j,l} = 2\sum_{g=1}^{8}\left[\sum_{j=5}^{8}\sum_{l=5}^{8} d_j^{(g)}\,d_{l+8}^{(g)}\,\{a_j(1)\,b_l(1) + b_l(1)\,a_j(1)\}\right]. \tag{10}$$

Equation (6) means the "total" intermolecular density as to the two systems, "total" implying the summation with respect to Eq. (7)–(10). Intermolecular part can be understood qualitatively by looking at the shaded region in Fig. 3. The existence of such density is essentially due to the overlapping of the non-orthogonal MO's between (I) and (II), and the integration of these quantities over all space of an electron 1 clarifies the physical meaning of the respective terms.

$\varrho(1\,|\,1)_{\text{exchange}}$ in Eq. (7) is the intermolecular density originated from the overlap of both occupied orbitals in (I) and (II), i.e. a_i and b_k. This exchange type of orbital interaction is expected to present the unfavorable density for the bond formation of the two BH_3 as shown in an example of the helium molecule [26].

Next $\varrho(1\,|\,1)_{\text{CT}}$ in Eq. (8) is the density due to the overlap between the occupied MO's in (I), a_i, and the unoccupied ones in (II), b_l. This term corresponds by nature to the product by the charge-transfer (CT) effect from a_i to b_l, in other words the electron jumping from (I) to (II).

$\varrho(1\,|\,1)_{\text{back CT}}$ in Eq. (9) has the reverse relation against $\varrho(1\,|\,1)_{\text{CT}}$, namely it is the density by the back CT from b_k of (II) to a_j of (I).

The last term, $\varrho(1\,|\,1)_{j,l}$, is the intermolecular density produced by the interaction between the both *unoccupied* MO's, a_j in (I) and b_l in (II). It may seem strange at first sight that the interaction of vacant orbitals yields the density. However in the method of the configuration analysis, the unoccupied state of a_j and b_l is the original one before the interaction occurs and at the system with the inclusion of the interaction between (I) and (II), a_j and b_l are no more *unoccupied* orbitals as shown later by the "occupancy of MO's in the interacting state" in Table 1. As a result of this influence, they have a little density to bear a part in the intermolecular component, $\varrho(1\,|\,1)_{j,l}$.

Thus we can get the partitioned form of the intermolecular (shaded part in Fig. 3) density, regarding diborane as the interacting two species. We will find the interesting and characteristic behavior of the MO's in two for making the *two-electron three-center bonds.*

4. Results

First in Fig. 4 the usual total density of diborane is depicted in the right half ($z>0$) of the $y-z$ plane ($x=0$). At the left half ($z<0$) in Fig. 4, the total density of one fragment, (I), is drawn (see Fig. 3). Especially in $y<0$ of Fig. 4, the change of (B H_b–B) → (B···H_b···B) is obviously observed. Hereafter we try to seek the reason of this drastic change in these two.

In Fig. 5 the density of $\varrho(1\,|\,1)_{\text{total}}$ in Eq. (6), cut in $y-z$ plane similarly as in the case of Fig. 4, is displayed concerning the intermolecular region (shaded part in Fig. 3). This shows that the bonding electron density between two are mainly localized along the direction from the boron atom of one fragment to H_b of the other, namely the introduction of the orbital interaction is found to present the new B···H_b density in favor of the formation of the three-center bonds from two BH_3. Direct B···B bond formation can not be observed so remarkably from this Figure, pointed out also by Burnelle and Kaufman [6]. As a whole, Fig. 5 is thought to indicate the *banana-bond* model so clearly as the result by the localized representation [13].

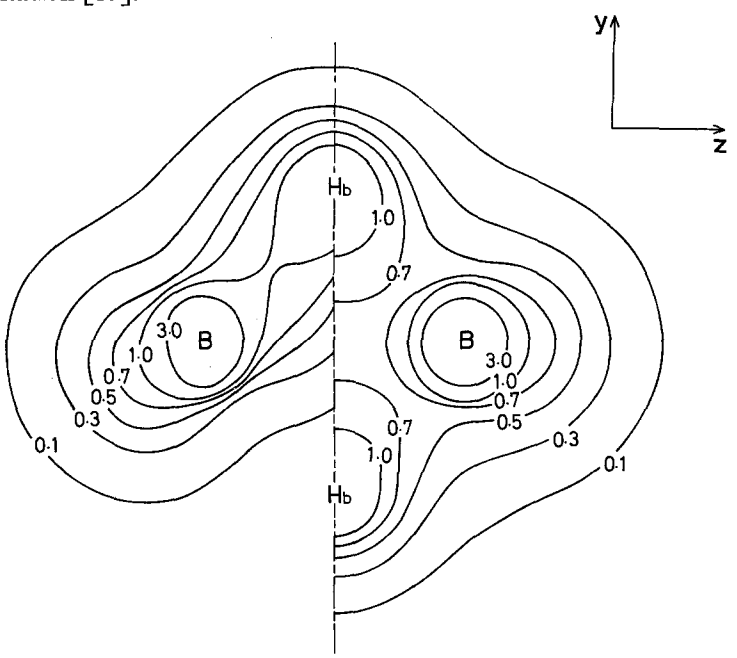

Fig. 4. The total electronic density map of the subsystem (I) at the left $\left(2\sum_{i=1}^{4}|a_i(1)|^2\right)$ and that of B_2H_6 at the right $\left(2\sum_{g=1}^{8}|\Psi_g(1)|^2\right)$. The values attached to the equal density lines are those given in $e/\text{Å}^3$

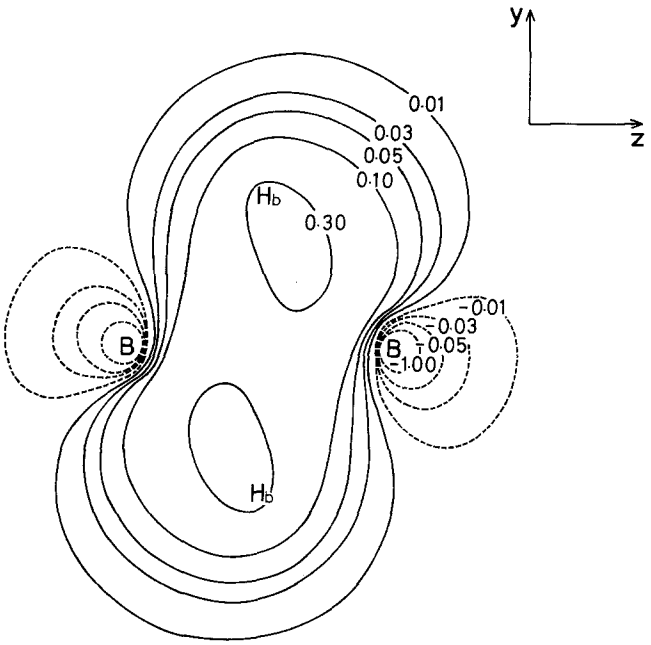

Fig. 5. The intermolecular electronic density map $\varrho(1\,|\,1)_{\text{total}}$ in Eq. (6)

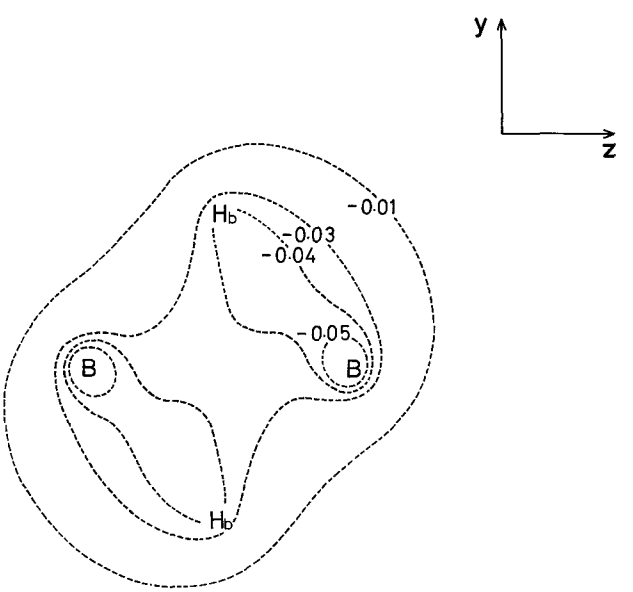

Fig. 6. The partial electronic density map by $\varrho(1\,|\,1)_{\text{exchange}}$ in Eq. (7)

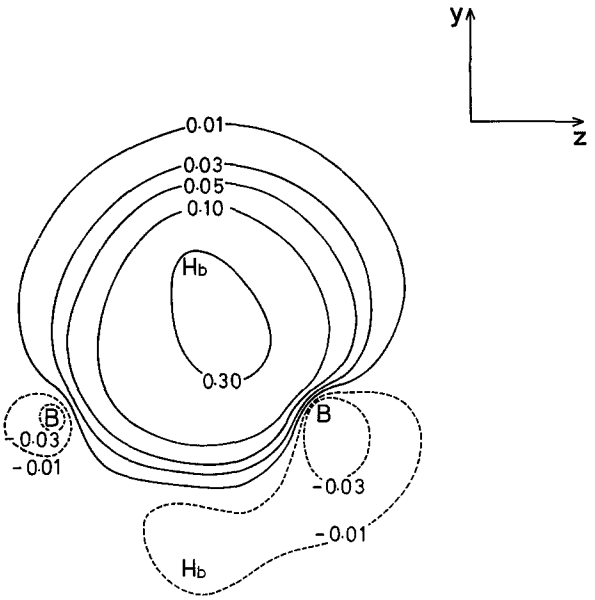

Fig. 7. The partial electronic density map by $\varrho(1\,|\,1)_{CT}$ in Eq. (8)

As one portion of $\varrho(1\,|\,1)_{total}$, Fig. 6 shows the electronic density by $\varrho(1\,|\,1)_{exchange}$ in Eq. (7). By looking at the negative equal density lines[2] in this Figure, we can make out the unfavorable operation of the interaction between both occupied orbitals for the bond formation [27] as predicted in the previous section. But the absolute value of the negative density in this Figure is not so large as the total one in Fig. 5 because of the lack in the effective overlap of the both occupied orbitals at the intermolecular region. At any rate this type of orbital *mixing* is by no means the major origin of the three-center bonds, and the *exchange* interaction operates to keep away each other BH_3 as expected by the analogy with He_2.

Next in Fig. 7 the electronic density by $\varrho(1\,|\,1)_{CT}$ of Eq. (8) is shown. This CT type is found to give the appreciable electron density to the intermolecular space of $y>0$ and to overcome the antibonding density produced by $\varrho(1\,|\,1)_{exchange}$, contributing considerably to the bonding component of $\varrho(1\,|\,1)_{total}$ in Fig. 5 ($H_b\cdots B$). Thus by this Figure we can see the important role of the overlap interaction of the CT mode upon the bond formation also in this "complex" [27].

$\varrho(1\,|\,1)_{CT}$ in Eq. (8) is the summed form as regards the pairs of i and l. Among the pairs, which plays the most dominant role of the CT interaction for such positive electron density at the upper ($y>0$) region? To obtain this information, we tentatively choose the matching of $i=4$ and $l=5$ from Eq. (8). That is, we take up the particular CT mode between the highest occupied (HO) MO in (I) and the lowest unoccupied (LU) MO in (II), termed here $\varrho(1\,|\,1)_{HO\to LU,CT}$ for convenience. In Fig. 8 the density by $\varrho(1\,|\,1)_{HO\to LU,CT}$ is drawn. We can see this is nearly the same map as that by $\varrho(1\,|\,1)_{CT}$, although the extension of the density line of Fig. 8 is a little reduced in scale compared with that of Fig. 7. Here, we come

[2] Hereafter the dotted lines are used so as to express the negative densities.

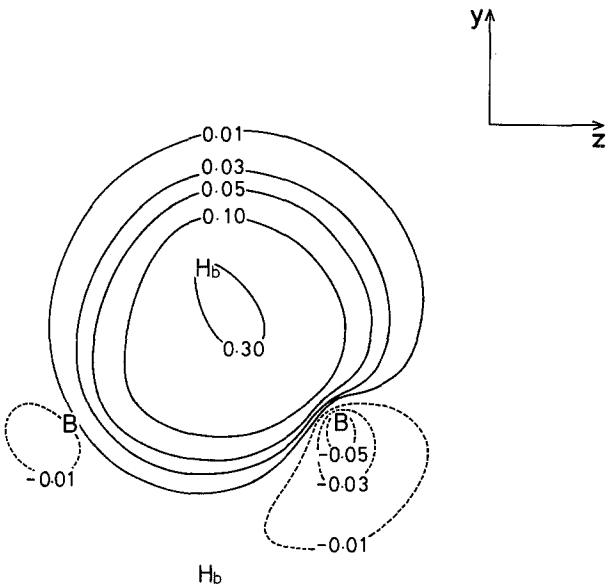

Fig. 8. The partial electronic density map by $\varrho(1\,|\,1)_{\mathrm{HO}\to\mathrm{LU,CT}}$

to the confirmation that the *particular* CT interaction is fairly important among the several pairs of MO's to explain the formation of the bridged bond ($H_b\cdots B$), and this CT interaction is originated from the overlap between the HOMO in (I) and the LUMO in (II).

To detect this overlap mode, we illustrate the density map of the HOMO in (I) subsystem in Fig. 9. From this Figure the HOMO is found to have the spatial extension along the $B-H_b$ direction, with its largest density on H_b. When the fragmental BH_3 is planar in D_{3h} symmetry which is calculated to be most stable geometry in its isolated state, this MO is degenerate with other one, both belonging to an irreducible representation, *E*. Then the MO is not so *active* as to interact effectively with the MO's in (II). But by the deformation of the planar BH_3 into that shown in Fig. 3, the character as an electron *donor* is increased in the fact that the energy level of the HOMO is lifted up to result in unstabilization, and furthermore that the lobe of the electron cloud grows larger toward H_b as pictured in Fig. 9.

On the other hand in Fig. 10, the extension of the LUMO in (II) is shown. In the planar D_{3h} symmetry of the BH_3, this MO is a pure *p* atomic orbital (AO) on the boron atom perpendicular to the molecular plane. The deformation of the BH_3 into the geometry of (II) in Fig. 3 gives the mixing of the *s*-type AO's and the enlargement of the density cloud toward H_b of (I) to this MO. Thus the spatial extension of the HOMO in (I) and the LUMO in (II) can overlap efficiently around the center of H_b in (I), and as a result the easiness of this particular CT interaction is brought about [28]. It is noteworthy that these MO's have just the same direction as that of the $B-H_b$ and $B\cdots H_b$, i.e. along the three-center bond. The dominance of this particular interaction will be understood more

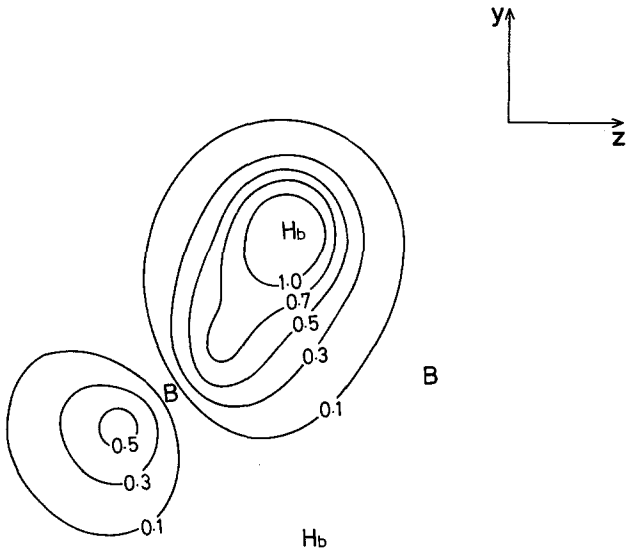

Fig. 9. The electronic density map of the HOMO in (I) BH_3 $\{2|a_4(1)|^2\}$

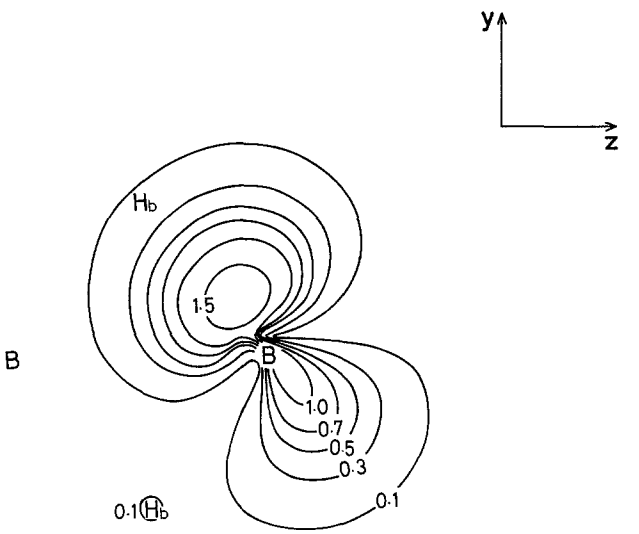

Fig. 10. The extension of the LUMO in (II) BH_3 $\{2|b_5(1)|^2\}$

directly by the comparison of the coefficients attached to several electronic configuration later [Eq. (11)].

As already seen, $\varrho(1\,|\,1)_{CT}$ or $\varrho(1\,|\,1)_{HO\to LU,CT}$ gives the positive and the effective electron density at the *upper* ($y>0$) region of the shaded part in Fig. 3. Then it is expected that the operation of the *back donation*, i.e. the reverse CT interaction from b_k in (II) to a_j in (I), will present the similar density to produce the lower ($y<0$) $B\cdots H_b$ bond in Fig. 3. To ascertain this point the density by $\varrho(1\,|\,1)_{\text{back CT}}$

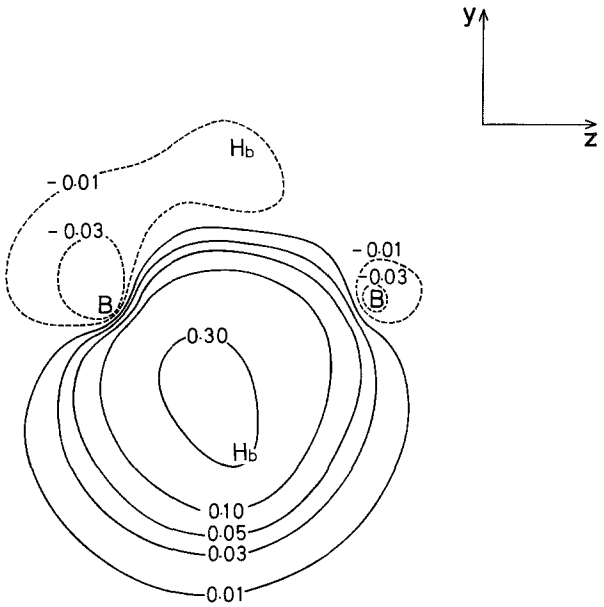

Fig. 11. The partial electronic density map by $\varrho(1\,|\,1)_{\text{back CT}}$ in Eq. (9)

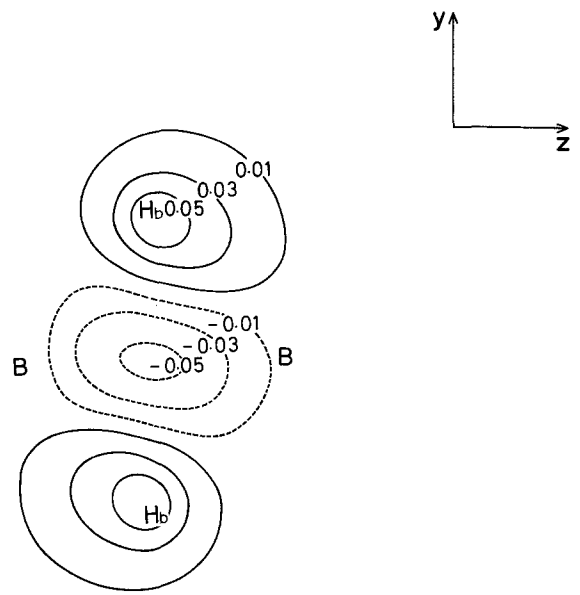

Fig. 12. The partial electronic density map by $\varrho(1\,|\,1)_{j,l}$ in Eq. (10)

is depicted in Fig. 11[3]. From this Figure also, the effective role of the back CT interaction between the occupied MO's in (II) (b_k) and the unoccupied ones in (I) (a_j) to form the lower B···H_b bond is elucidated as expected.

[3] This is completely the same map as the one in Fig. 7 when rotated through 180° about x axis. This is because the two B...H_b bonds are placed in C_{2h} symmetry.

Table 1. The occupancy of MO's of one BH_3 (I) before and after the orbital interaction

The MO's of (I) in Fig. 2	Before	After
$a_8 (=b_8)$	0	0.0057
$a_7 (=b_7)$	0	0.0050
$a_6 (=b_6)$	0	0.0344
$a_5 (=b_5)$ the LUMO	0	0.5412
$a_4 (=b_4)$ the HOMO	2	1.5270
$a_3 (=b_3)$	2	1.9943
$a_2 (=b_2)$	2	1.8914
$a_1 (=b_1)$	2	2.0011

In Fig. 12 the density by $\varrho(1\,|\,1)_{j,l}$ of Eq. (10) is shown. There, the preferable positive electron density to the bond formation of B···H_b and the negative B···B density can be observed, although the amount of the former is far smaller than that by $\varrho(1\,|\,1)_{\mathrm{CT}}$ and $\varrho(1\,|\,1)_{\mathrm{back\,CT}}$. Here Fig. 6 and Fig. 12 demonstrate the direct B···B bond is interfered with by the orbital interaction originated from $\varrho(1\,|\,1)_{\mathrm{exchange}}$ and $\varrho(1\,|\,1)_{j,l}$ respectively, but the antibonding component of the B···B bond is overcome easily by the large CT effect, shown as a result in $\varrho(1\,|\,1)_{\mathrm{total}}$ of Fig. 5. At any rate the existence of the direct B···B bond does not seem the essential factor for the formation of the B_2H_6 molecule.

In Table 1 *the occupancy of the MO's* [18] in one fragment is tabulated before and after the orbital interaction, where the notations attached to the MO's are the ones in Fig. 2. Looking at these results, we find that the orbital mixings change the *occupancy*, particularly in the decrease of the density of the HOMO and at the same time in the new occupation of the considerable density of LUMO. These changes are, of course, attributable seriously to the special orbital interactions between the HOMO in one subsystem and the LUMO in the other as mentioned before. So the migration of the electronic density is almost through these orbitals. The decreased value in a_2 (or b_2) MO (2→1.8914) is due to the moderate overlap against the LUMO in the other BH_3. The density at the intermolecular region is yielded mainly by the electron jumping through such particular orbital interactions.

The most obvious feature of the orbital interaction is given by the use of the configuration analysis as follows;

$$
\begin{aligned}
\Psi = {} & \mathbf{0.2984}\,\Psi_0 \\
& + \mathbf{0.1950}\,\Psi(a_4 \to b_5) + 0.0338\,\Psi(a_4 \to b_6) + 0.0526\,\Psi(a_2 \to b_5) \\
& + \mathbf{0.1950}\,\Psi(b_4 \to a_5) + 0.0338\,\Psi(b_4 \to a_6) + 0.0526\,\Psi(b_2 \to a_5) \\
& + 0.0378\,\Psi(a_2 \to a_5) + 0.0217\,\Psi(a_4 \to a_5) + 0.0388\,\Psi(a_4 \to a_6) + 0.0181\,\Psi(a_4 \to a_7) \\
& + 0.0378\,\Psi(b_2 \to b_5) + 0.0217\,\Psi(b_4 \to b_5) + 0.0388\,\Psi(b_4 \to b_6) + 0.0181\,\Psi(b_4 \to b_7) \qquad (11) \\
& + 0.0238\,\Psi(a_2 \to b_5, a_4 \to b_5) + 0.0510\,\Psi(a_4 \to b_5, a_4 \to b_5) + 0.0138\,\Psi(a_4 \to b_5, a_4 \to b_6) \\
& + 0.0238\,\Psi(b_2 \to a_5, b_4 \to a_5) + 0.0510\,\Psi(b_4 \to a_5, b_4 \to a_5) + 0.0138\,\Psi(b_4 \to a_5, b_4 \to a_6) \\
& + 0.0288\,\Psi(a_2 \to b_5, b_4 \to a_5) + 0.0288\,\Psi(b_2 \to a_5, a_4 \to b_5) \\
& + 0.0195\,\Psi(a_4 \to b_6, b_4 \to a_5) + 0.0195\,\Psi(b_4 \to a_6, a_4 \to b_5) \\
& + \mathbf{0.1050}\,\Psi(a_4 \to b_5, b_4 \to a_5) + \cdots .
\end{aligned}
$$

There, Ψ denotes the ground state of B_2H_6 expressed by Ψ_g in Eq. (2). Ψ_0 stands for the adiabatic interacting state retaining the original electronic structure in two fragmental parts. The other terms in the right side of Eq. (11) mean the electronic states with some electron jumping. For instance, $\Psi(a_4 \rightarrow b_5)$ is the mono-transferred state from a_4 MO (HOMO) in (I) to b_5 MO (LUMO) in (II). $\Psi(a_2 \rightarrow a_5)$ is the mono-excited state in (I) from a_2 to a_5. $\Psi(a_2 \rightarrow b_5, a_4 \rightarrow b_5)$ is the di-transferred state from a_2 in (I) to b_5 in (II) and at the same time from a_4 in (I) to b_5 in (II), and $\Psi(a_2 \rightarrow b_5, b_4 \rightarrow a_5)$ is the di-transferred state mutually between the MO's in the two fragments. The coefficients (absolute values) attached to Ψ_0 and $\Psi(\cdots)$ can be obtained by the above mentioned technique. In this Equation the "symmetry-forbidden" electron transferred or excited states, caused by the orbital interaction between the MO's of the different symmetry groups (A and S), are not listed because the contribution of such states to Ψ is completely zero. Among the terms in Eq. (11), the numerical coefficients of the major ones are written in the bold face for notice. Here the excited states such as $\Psi(a_2 \rightarrow a_5)$ and $\Psi(b_4 \rightarrow b_5)$ are found to be less important than the others. We can see the notable terms except Ψ_0 correspond to the before mentioned CT interacting state from HOMO (a_4 and b_4) to the LUMO (a_5 and b_5). Furthermore the unexpectedly small coefficient of Ψ_0 (0.2984) is owing to the fact that the CT ($a_i \rightarrow b_l$) and the back CT ($b_k \rightarrow a_j$) interactions work cooperatively to give electrons enough activeness to jump from the originally occupied MO's (a_i and b_k) into the originally unoccupied ones (a_j and b_l). This remarkable role of the CT and the back CT interactions for the three-center bonds can be understood also from the inspection of the larger values (0.1050) attached to $\Psi(a_4 \rightarrow b_5, b_4 \rightarrow a_5)$ than expected. This state stands for the mutual HOMO-LUMO interaction. So we obtain the same conclusion as stated by the use of the density maps, that the HOMO-LUMO CT interaction is fairly important for describing the electronic structure in the "complex" by two BH_3, i.e. B_2H_6.

5. Conclusive Discussion

In this work the electronic structure of diborane which is thought an *electron-deficient molecule* has been studied by the technique regarding the molecule as the product of the two interacting fragments. This method, in other words, deals with the structural problem of the molecule as if it were a charge-transfer complex of the Mulliken type [29], $BH_3 \ldots BH_3$.

Here it is easily understood that the *monomer* (BH_3) acts as an electron *acceptor* by the following reason. That is, if the monomer stayed at the planar geometry in D_{3h} symmetry, it has a pure and vacant p AO perpendicular to the plane apt to accept the charge density considerably, as shown by an example that $NH_3 \cdot BH_3$ is a typical model of the charge-transfer complex [18]. This *electrophilic* ability of the monomer is not so weakened by some deformation of the planar geometry, and in the case of the configuration of one monomer (II) shown in Fig. 3, the *electrophilic* character is rather increased toward H_b in the other monomer (I) as illustrated in Fig. 10.

But on the other hand, it may seem curious that the monomer plays a role as an electron *donor* as well as an *acceptor*, for it has 8 electrons (*two* almost

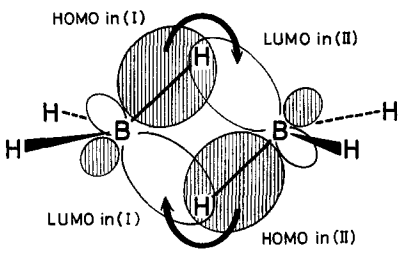

Fig. 13. A schematic representation of the electronic density distribution by the particular orbital interaction

localized in 1*s* shell and *six* used for three B–H σ bonds), without excessive electrons to form, for example, a lone pair of them. Therefore, if the monomer left undeformed at the D_{3h} structure or nearly so, the electron donating character might be weak. From these inspections it can be interpreted that diborane in its ground state does not retain the ethane-like structure, for the efficient donative operation in each BH_3 is absent. So the structural deformation of one monomer is necessary to make it donative, in other words, to produce the *active* occupied MO against the LUMO of the other monomer. This request of the structural change for the ease of the *particular* orbital interaction is satisfied by the appropriate deformation of the two monomers in Fig. 3 from D_{3h} symmetry. This results in the production of the *active* MO, i.e., the HOMO, in Fig. 9 and then in the appearance of the appreciable charge density at the intermolecular region by the overlap interaction.

Thus we could say that the bridged structure of B_2H_6 is born by the deformation of the D_{3h} monomers for the purpose that each plays the role as a *donor* rather than an *acceptor* in the B_2H_6 *complex*. We can observe that the HOMO and the LUMO of the respective monomers have their spatial extension coinciding with that of $B-H_b$ bonds, which results in the maximum values of their overlap on the center of the two bridge hydrogens.

Finally the last picture, exhibiting the density distribution schematically, seems to express our insistence.

Acknowledgement. One of the authors (S.Y.) is indebted to Professor Hiroshi Kato, Mr. Kazuhiro Ishida and Mr. Shigeki Kato for their invaluable advices.

We wish to express our appreciation to the Data Processing Center of Kyoto University for generous permission to use the FACOM 230-60 computer.

References

1. Lipscomb, W.N.: J. Chem. Phys. **22**, 985 (1954)
2. Eberhardt, W.H., Crawford, Jr., B., Lipscomb, W.N.: J. Chem. Phys. **22**, 989 (1954)
3. Hoffmann, R., Lipscomb, W.N.: J. Chem. Phys. **37**, 2872 (1962)
4. Boer, F.P., Newton, M.D., Lipscomb, W.N.: J. Am. Chem. Soc. **88**, 2361 (1966)
5. Hamilton, W.C.: Proc. Roy. Soc. (Lond.) A**235**, 395 (1956)
6. Burnelle, L., Kaufman, J.J.: J. Chem. Phys. **43**, 3540 (1965)
7. Buenker, R.J., Peyerimhoff, S.D., Allen, L.C., Whitten, J.L.: J. Chem. Phys. **45**, 2835 (1966)
8. Palke, W.E., Lipscomb, W.N.: J. Chem. Phys. **45**, 3948 (1966)

9. Yamazaki, M.: J. Chem. Phys. **27**, 1401 (1957)
10. Laws, E. A., Stevens, R. M., Lipscomb, W. N.: J. Am. Chem. Soc. **94**, 4461 (1972)
11. Gimarc, B. M.: J. Am. Chem. Soc. **95**, 1417 (1973)
12. Adamson, G. W., Linnett, J. W.: J. Chem. Soc. (A) **1969**, 1697.
13. Switkes, E., Stevens, R. M., Lipscomb, W. N.: J. Chem. Phys. **51**, 2085 (1969)
14. Gelus, M., Ahlrichs, R., Staemmler, V., Kutzelnigg, W.: Chem. Phys. Letters **7**, 503 (1970)
15. Baylis, A. B., Pressley, Jr., G. A., Stafford, F. E.: J. Am. Chem. Soc. **88**, 2428 (1966)
16. Mappes, G. W., Fridmann, S. A., Fehlner, T. P.: J. Phys. Chem. **74**, 3307 (1970)
17. Baba, H., Suzuki, S., Takemura, T.: J. Chem. Phys. **50**, 2078 (1969)
18. Fujimoto, H., Kato, S., Yamabe, S., Fukui, K.: J. Chem. Phys. (in press).
19. Morita, H., Nagakura, S.: Theoret. Chim. Acta (Berl.) **27**, 325 (1972)
20. Roothaan, C. C. J.: Rev. Mod. Phys. **23**, 69 (1951)
21. Hehre, W. J., Stewart, R. F., Pople, J. A.: J. Chem. Phys. **51**, 2657 (1969)
22. O-ohata, K., Taketa, H., Huzinaga, S.: J. Phys. Soc. Japan **21**, 2306 (1966)
23. Taketa, H., Huzinaga, S., O-ohata, K.: J. Phys. Soc. Japan **21**, 2313 (1966)
24. Stewart, R. F.: J. Chem. Phys. **52**, 431 (1970)
25. Bartell, L. S., Carroll, B. L.: J. Chem. Phys. **42**, 1135 (1965)
26. Gentile, G.: Z. Physik **63**, 795 (1930)
27. Fukui, K., Fujimoto, H., Yamabe, S.: J. Phys. Chem. **76**, 232 (1972)
28. Fukui, K., Fujimoto, H.: Bull. Chem. Soc. Japan **42**, 3399 (1969)
29. Mulliken, R. S.: J. Am. Chem. Soc. **74**, 811 (1952)

Dr. Sh. Yamabe
Department of Hydrocarbon Chemistry
Faculty of Engineering
Kyoto University
Kyoto, Japan